Electronic Supplementary Information (ESI)

Cu^{2+}-modulated in situ growth of quantum dots for split-type photoelectrochemical immunoassay of prostate specific antigen

Yang Zang,[a]* Yun Ju,[a] Jingjing Jiang,[a]* Qin Xu,[a] Ming Chu[b] and Huaiguo Xue[a]

[a] School of Chemistry and Chemical Engineering, Yangzhou University, Yangzhou, 225002, Jiangsu, China.

[b] The First Affiliated Hospital with Nanjing Medical University, Nanjing, Jiangsu, 210029, P. R. China

*Corresponding author. Tel.: +86-514-87975436 / Fax: +86-514-87975244.

E-mail address: zangyang@yzu.edu.cn, jjj@yzu.edu.cn.

Experimental section

Apparatus

Scanning electron micrograph (SEM) was characterized using S-4800 field emission scanning electron microscopy (Hitachi, Japan). Transmission electron micrographs (TEM) were performed by a Tecnai 12 microscope (Philips, Netherlands). UV–vis absorption spectra were obtained by a UV-2501PC spectrometer (Shimadzu Co. Kyoto, Japan). Fluorescence (FL) measurements were conducted on an F-4500 fluorescence spectrometer (Hitachi, Japan) equipped with a xenon lamp. X-ray photoelectron spectroscopy (XPS) measurements were carried out on an ESCALAB 250Xi spectrometer (Thermo Fisher, USA) with an Al *K*α radiation source. Raman spectrum was performed by a DXRxi Micro Raman imaging spectrometer (Thermo Fisher, USA).

Dynamic light scattering (DLS) spectrum was obtained via Nano-ZS90 light scattering instrument (Malvern, Britain). High mass accuracy ESI spectra were recorded on an ultrahigh-resolution ESI-Time-of-Flight with Bruker Daltonik maxis (Bremen, Germany). Incident-photon-to-current conversion efficiency (IPCE) data were measured in the wavelength range from 300 to 800 nm (Newport 94063, Stratford, CT, USA). Current-voltage (I-V) experiments were recorded by a CHI 660E electrochemical workstation (CH Instruments Inc., USA). Photoelectrochemical measurements were performed via a home-built PEC system with white light as an accessory excitation source. Electrochemical impedance spectroscopy (EIS) was tested using a PGSTAT30/FRA2 system (Autolab, The Netherlands). All experiments were carried out at room temperature using a conventional three-electrode system: a modified ITO electrode (4 mm in diameter) as the working, a platinum electrode as the auxiliary, and an Ag/AgCl as the reference electrodes.

Preparation of MoS_2 QDs

MoS_2 QDs were prepared by supersonic assisted liquid exfoliation technique.[S1] Briefly, 300 mg of MoS_2 powder was dispersed into 100 mL ethanol/water solution (the volume fraction of water was 55%), and then sonicated for over 24 h. The above dispersion was centrifuged for 20 min thrice at 6000 rpm to remove the unexfoliated bulk MoS_2. The resulting supernatant was further collected via a vacuum-rotary evaporation procedure at 60 °C under reduced pressure. After being

dissolved in deionized water and filtered by 0.22 μm ultrafiltration membrane, the obtained aqueous solution of MoS_2 QDs was stored at 4 °C for next experiments.

Preparation of CuO-Ab_2 conjugates

CuO-Ab_2 conjugates were prepared according to a previous report.[S2] Firstly, 1 mg of CuO NPs was dispersed into 1 mL of 0.01 M phosphate buffer saline (PBS) of pH 7.4 followed by ultrasonic treatment for 10 min, and vortexed the mixture for 3 h at 500 rpm after the addition of 500 μL Ab_2 with a concentration of 0.048 mg mL^{-1}. Subsequently, the resulting solution was centrifuged for 10 min at 10000 rpm to remove the unlabeled Ab_2 in the supernatant, whereas the precipitated CuO-Ab_2 conjugates were redispersed in 1.5 mL PBS and centrifuged for 10 min again at 5000 rpm to rid the excess precipitate of CuO NPs. Finally, 200 μL of 0.01 M PBS of pH 7.4 containing 10% BSA was added and vortexed for 30 min to stabilize the obtained CuO-Ab_2 solution, which was stored at 4 °C for further use.

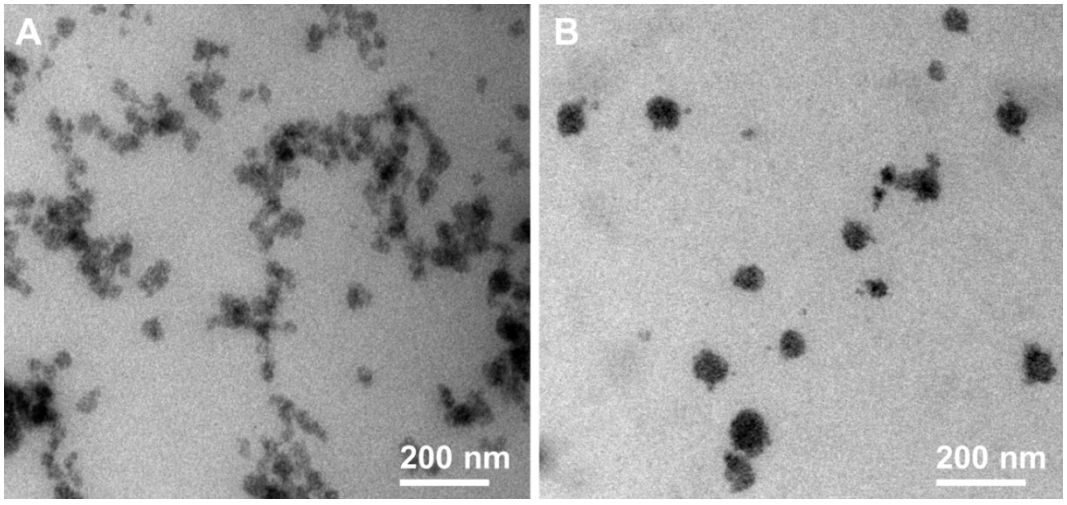

Fig. S1 TEM images of (A) CuO NPs and (B) CuO-Ab_2 conjugates.

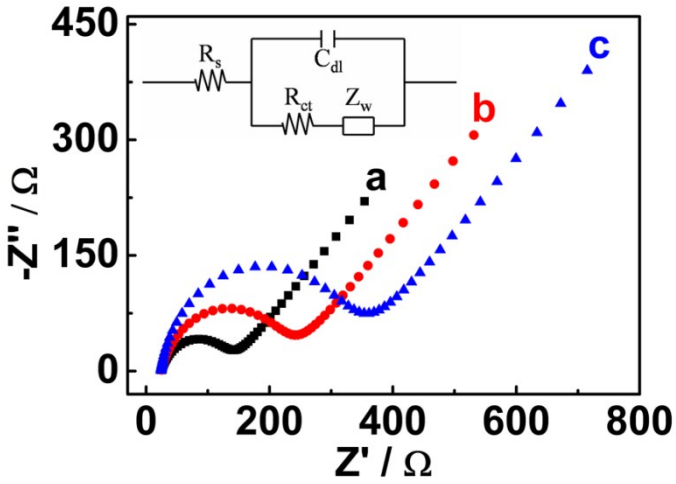

Fig. S2 EIS of bare ITO (a), MoS_2/ITO (b), and CdS/MoS_2/ITO (c) electrodes in 0.1 M Na_2SO_4 solution containing 5 mM $[Fe(CN)_6]^{3-/4-}$. The applied potential is 0.180 V with the signal amplitude of 5 mV, and the frequency range is 0.1 Hz−100 kHz. Inset: the electrical equivalent circuit applied to fit the impedance data; R_s, Z_w, R_{ct}, and CPE represent the Ohmic resistance of the electrolyte, Warburg impedance, charge-transfer resistance, and constant phase angle element, respectively.

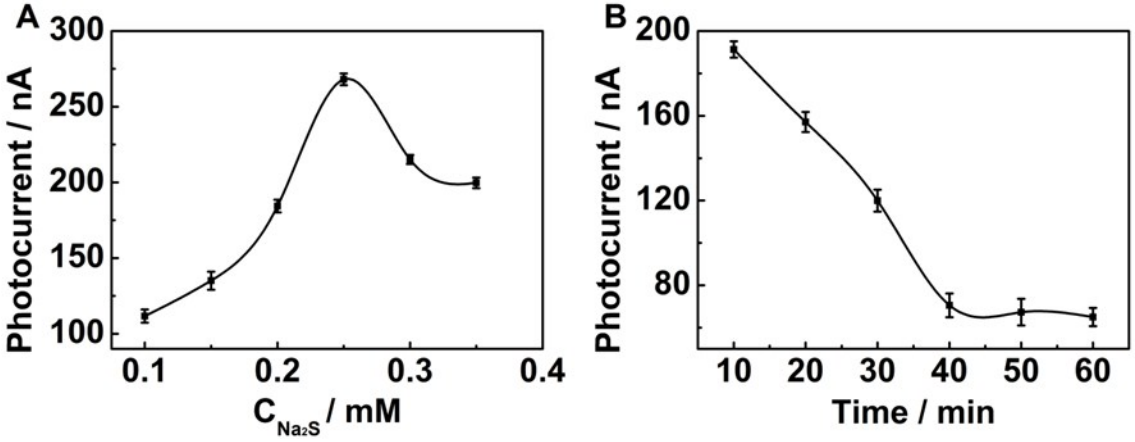

Fig. S3 (A) Effect of Na_2S concentration on the photocurrent response of in situ generation CdS QDs-modified MoS_2/ITO electrode. (B) Effect of incubation time of PSA with Ab_1 on the photocurrent response of designed immunosensor in the presence of 10 ng mL^{-1} PSA.

Table S1 Comparison of the analytical performance of various immunoassay methods for PSA detection.

Detection method	Linear range (ng mL^{-1})	Detection limit (ng mL^{-1})	References
Electrochemistry	1.5×10^{-2} – 8.0	1.7×10^{-3}	S3
Electrochemistry	5.0×10^{-4} – 10	1.2×10^{-4}	S4
Electrochemiluminescence	5.0×10^{-4} – 5.0	1.7×10^{-4}	S5
Electrochemiluminescence	1.0×10^{-4} – 50	5.6×10^{-5}	S6
Electrochemiluminescence	1.0×10^{-5} – 10	5.0×10^{-6}	S7
Fluorescence	1.0×10^{-3} – 20	3.0×10^{-4}	S8
Fluorescence	1.0×10^{-3} – 1.0	3.0×10^{-4}	S9
Raman scattering	1.0×10^{-3} – 10	6.5×10^{-4}	S10
Photoelectrochemistry	5.0×10^{-3} – 50	2.6×10^{-3}	S11
Photoelectrochemistry	1.0×10^{-2} – 20	3.8×10^{-3}	S12
Photoelectrochemistry	5.0×10^{-4} – 10	2.9×10^{-4}	This work

Table S2 Detection results and recoveries of PSA in human serum samples.

Sample	Reference method (ng mL^{-1})	Added (ng mL^{-1})	Proposed method (ng mL^{-1})	RSD (%, n=5)	Recovery (%, n=5)
1	0.54	0	0.50	7.12	-
		2.0	2.65	6.55	105.5
		4.0	4.63	5.82	102.3
		6.0	6.45	5.09	98.5
2	1.12	0	1.19	5.17	-
		2.0	3.07	4.19	97.5
		4.0	4.98	5.56	96.5
		6.0	7.19	6.05	101.2

References

S1 K. G. Zhou, N. N. Mao, H. X. Wang, Y. Peng and H. L. Zhang, *Angew. Chem. Int. Ed.*, 2011, **50**, 10839–10842.

S2 Q. F. Xie, X. H. Weng, L. J. Lu, Z. Y. Lin, X. W. Xu and C. L. Fu, *Biosens. Bioelectron.*, 2016, **77**, 46–50.

S3 Y. X. Hao, P. D. Yan, X. Zhang, H. W. Shen, C. L. Gu, H. Q. Zhang, M. H. Zhang and H. Xiang, *Microchim. Acta*, 2017, **184**, 4341–4349.

S4 X. Zhou, L. Yang, X. P. Tan, G. F. Zhao, X. G. Xie and G. B. Du, *Biosens. Bioelectron.*, 2018, **112**, 31–39.

S5 J. Cao, J. J. Yang, L. Z. Zhao, Y. L. Wang, H. Wang, Y. M. Liu and S. H. Ma, *Biosens. Bioelectron.*, 2018, **99**, 92–98.

S6 L. Yang, Y. Y. Li, Y. Zhang, D. W. Fan, X. H. Pang, Q. Wei and B. Du, *ACS Appl. Mater. Interfaces*, 2017, **9**, 35260–35267.

S7 W. J. Zhu, M. S. Khan, W. Cao, X. Sun, H. M. Ma, Y. Zhang and Q. Wei, *Biosens. Bioelectron.*, 2018, **99**, 346–352.

S8 H. M. Pei, S. Y. Zhu, M. H. Yang, R. M. Kong, Y. Q. Zheng and F. L. Qu, *Biosens. Bioelectron.*, 2015, **74**, 909–914.

S9 L. F. Yang, N. Li, K. Wang, X. M. Hai, J. X. Liu and F. Q. Dang, *Talanta*, 2018, **179**, 531–537.

S10 L. L. Xie, X. Yang, Y. He, R. Yuan and Y. Q. Chai, *ACS Appl. Mater. Interfaces*, 2018, **10**, 15200–15206.

S11 X. P. Wang, R. Xu, X. Sun, Y. G. Wang, X. Ren, B. Du, D. Wu and Q. Wei, *Biosens. Bioelectron.*, 2017, **96**, 239–245.

S12 K. Y. Zhang, S. Z. Lv, Z. Z. Lin and D. P. Tang, *Biosens. Bioelectron.*, 2017, **95**, 34–40.